Contents

List of Figures

List of Tables

1 NEFI

1.1 abstract

Networks are amongst the central building blocks of many systems. Given a graph of a network, methods from graph theory enable a precise investigation of its properties. Software for the analysis of graphs is widely available and has been applied to study various types of networks. In some applications, graph acquisition is relatively simple. However, for many networks data collection relies on images where graph extraction requires domain-specific solutions. Here we introduce NEFI, a tool that extracts graphs from images of networks originating in various domains. Regarding previous work on graph extraction, theoretical results are fully accessible only to an expert audience and ready-to-use implementations for non-experts are rarely available or insufficiently documented. NEFI provides a novel platform allowing practitioners to easily extract graphs from images by combining basic tools from image processing, computer vision and graph theory. Thus, NEFI constitutes an alternative to tedious manual graph extraction and special purpose tools. We anticipate NEFI to enable time-efficient collection of large datasets. The analysis of these novel datasets may open up the possibility to gain new insights into the structure and function of various networks. NEFI is open source and available at http://nefi.mpi-inf.mpg.de.

1.2 introduction

The study of complex network-like objects is of increasing importance for many scientific domains. The mathematical study of networks, Graph Theory, formalizes a network's structure by modeling the constituents of a network as *vertices* and the pairwise relations between them as *edges*. Some communities traditionally refer to vertices as nodes or sites and to edges as arcs or links. Networks are ubiquitous in everyday life. Examples are as diverse as the Internet, social networks, transportation networks, metabolic networks, blood vessels or the vein networks of leaves. For a comprehensive review see [17].

In situations where the extraction of a mathematical graph from a physical network is easy, the size of graphs that can be analyzed quickly increased from hundreds to millions of vertices. At the same time it became feasible to build large

databases of various types of networks. This enabled the application of software incorporating methods from statistics and graph theory to obtain many results that changed our understanding of large scale network structures. However, digitization remains difficult for many types of networks, e.g. leaf venations, blood vessels or food webs, and therefore ready-to-analyze datasets are often not available. In these cases, investigation on a larger scale requires tedious and sometimes error prone data acquisition.

In many experimental settings networks are initially available as high quality images obtained under laboratory control. Before any analysis can take place, it is necessary to extract the associated graphs from these images. This requires the identification of vertices and edges within the depicted structure. This process can quickly become very work-intensive even for smaller networks, which makes automated solutions indispensable.

Leveraging advances in computer vision, several authors have proposed and successfully implemented solutions for domain specific graph extraction applications. The authors of [18], [19] consider the mycelial networks of *P. impudicus*. They use watershed segmentation in combination with a novel enhancement step designed to highlight curvilinear features in the input networks. Based on the segmented image a skeleton is computed and used to extract the graph representing the input network. The resulting method is designed to be brightness and contrast invariant in order to correctly extract the networks grown by *P. impudicus* from challenging noisy or low contrast images.

Baumgarten et al. [4], [5] investigate the vein networks of *P. polycephalum*. For segmenting the input image they rely on careful constant thresholding followed by a sequence of restoration algorithms that try to repair the network in the segmented image. Next, the restored segmented image is used to compute a skeleton. After applying another sequence of correction steps, the skeleton is scanned to extract the graph of the input network.

In [7] a more general algorithm applicable to a variety of problems is proposed. Based on an original stochastic model, the authors use Monte Carlo sampling to obtain junction-points in the input image. This technically involved solution guarantees structural coherence for the resulting graph representation. Further examples include the extraction of road networks [16], retinal blood vessel analysis [12] and the extraction of plane graphs [21].

The three above mentioned algorithmic solutions for the network extraction problem exhibit one or more of the following limitations:

- They do not build on top of well-established computer vision methods and tend to rely on ad-hoc algorithms. As a result the quality of the method and its implementation could likely be improved. In addition, a lot of time is spent on reimplementing algorithms that are already available.

- They are not implemented or only available as pseudo-code.
- They are implemented but not designed for easy of use, distribution and extendability.

We are aware that the primary objective of the work cited above is not the production of reusable software, but of algorithms and tools for solving a concrete research question. As a result, the above authors have limited time for researching advances in computer vision, following best software engineering practice or writing documentation respectively.

From experience we know that when producing an easy-to-use software, a large part of the required work consists of specifying and improving the user-interface as well as working out minor bugs and annoyances. This type of work, while time consuming, is essential for any software aiming to reach a non-negligible audience. However, efforts like these are hardly attractive to researchers whose focus is on obtaining the next result. While we understand that under these circumstances the aforementioned limitations arise naturally, we strongly believe that it is necessary to overcome those limitations in order to increase the value and the impact of scientific software in general and network extraction software in particular.

To this end, we introduce NEFI, a lightweight piece of ready-to-go software intended to enable the non-expert to automatically extract networks from images. NEFI constitutes an extensible framework of interchangeable algorithms accessible through an intuitive graphical user interface.

We emphasize at this point that we do not claim to introduce novel techniques for image processing or computer vision. Instead, our contribution consists of a reusable, flexible and easily extendable toolbox combining well-known methods, which have become standard in their respective fields of origin, in a meaningful way. By introducing NEFI, we hope to make these methods more widely accessible to practitioners in other fields.

NEFI's segmentation is based on a combination of standard routines available in OpenCV, (2015), [6]. These algorithms are known to perform well on clean and uncluttered images obtained under controlled laboratory conditions. However, on more challenging inputs of low contrast, strong gradients or similar irregularities, their performance is severely reduced. Nevertheless, in these cases more involved algorithms, currently not implemented as part of a reliable library and thus not integrated into NEFI, may still be able to process these images. To help meet this situation, NEFI was designed with extendability in mind. As a result users will find it easy to build on-top of NEFI's code in order to add their own implementations of more sophisticated methods.

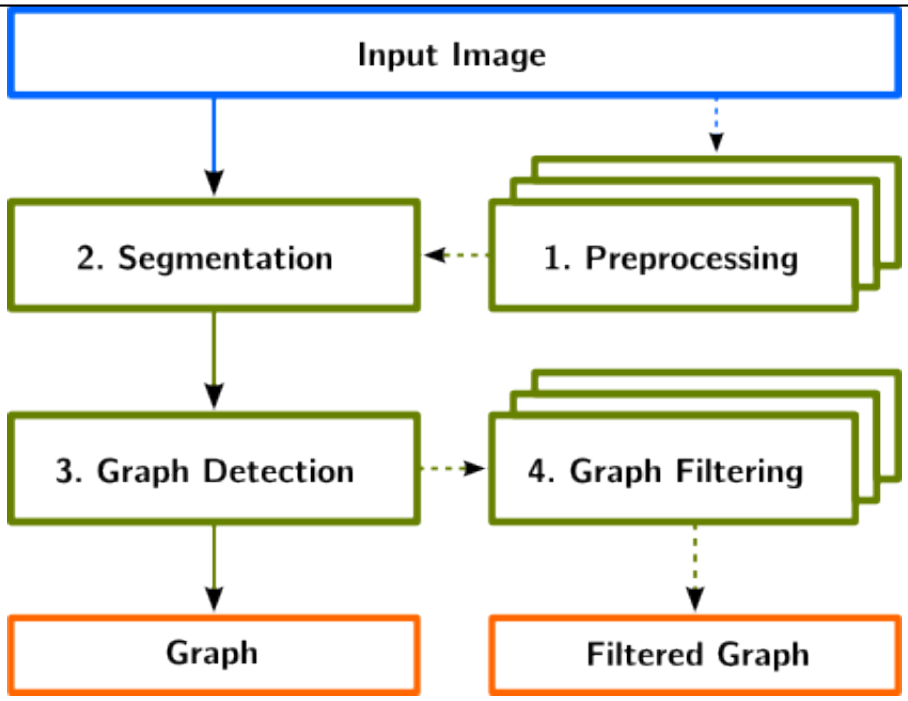

Figure 1.1: A flow chart illustrating NEFI's pipeline components in green boxes. Dashed arrows depict optional sections of the pipeline. Blue and orange boxes denote NEFI's input and possible outputs respectively.

1.3 Network Extraction From Images

NEFI features a collection of image processing routines, segmentation methods and graph algorithms designed to process 2D digital images of various networks and network-like structures. Its main function is executing a so-called extraction pipeline, designed to analyze the structures depicted in the input image. An extraction pipeline, for short pipeline, denotes an ordered sequence of algorithms. A successful execution will return a representation of the network in terms of an edge-weighted undirected planar graph. Computed weights include edge lengths and edge widths. Once the graph is obtained, available graph analysis software [2], [3], [10], [13], [14], [23] or custom written scripts can be deployed to investigate its properties.

A typical pipeline combines algorithms from up to four different classes: preprocessing, segmentation, graph detection and graph filtering, see Figure 1.1. A more detailed description follows below.

For each pipeline section, NEFI typically offers several interchangeable algorithms to choose from. After executing preprocessing routines, a segmentation algorithm separates foreground from background. Then the foreground is thinned

to a skeleton from which the vertices and edges of the graph are determined. In the process various edge weights are computed. Finally, the graph can be subjected to a variety of useful graph filters. Figure 1.2 illustrates the intermediate results of NEFI's pipeline steps listed in the order of their execution. When a pipeline is executed, NEFI makes all intermediate results available via its clean and intuitive GUI, see Figure 1.3.

Using the GUI all basic functions of NEFI can be accessed in an intuitive fashion. To facilitate ease-of-use, most of NEFI's algorithms come with default parameters based on the settings in OpenCV [6], which were found to perform well on our test sets as well as on many other images.

There are various predefined pipelines to get started immediately. Alternatively, users may freely combine the various methods to build custom pipelines. Both approaches allow the user to experiment with the available methods in order to close in on the optimal settings for the data. Once a pipeline is constructed, it can be saved and reused. NEFI's simple pipeline concept together with a self-explanatory graphical user interface make working with NEFI intuitive and straightforward. NEFI also offers a command-line mode, which is suited for batch processing.

NEFI comes with a number of example images from different domains which we use to produce the figures in this work. Figure 1.4 and Figure 1.5 show NEFI's output on two images using predefined pipelines. Blue squares denote the vertices and red lines the edges of the detected graph. The thickness of the detected edges corresponds to thickness of the depicted structures. For comparison the extracted graph is drawn on top of the input image. We present a detailed quantitative evaluation in a later section.

We stress that NEFI can deal with a range of inputs from various domains as long as they are of sufficient quality. In addition to the examples shown above, it has been successfully used to process images of natural (e.g. leaf venation, patterns of mud cracks) as well as man-made structures (tilings). It is also straightforward to add custom extensions. We provide a well documented platform which allows programmers to include more specialized segmentation algorithms or additional graph filters. For an overview of alternative graph extraction approaches see for example [8].

Next, we discuss the purpose and design of each major stage of the pipeline and highlight some of NEFI's strong points.

1.3.1 Preprocessing Collection

The preprocessing section of the pipeline offers various standard image processing algorithms intended to be used prior to the segmentation step. Preprocessing methods may be exploited to affect the output of the segmentation step. For example, adding a slight blur to an input image may benefit the overall result

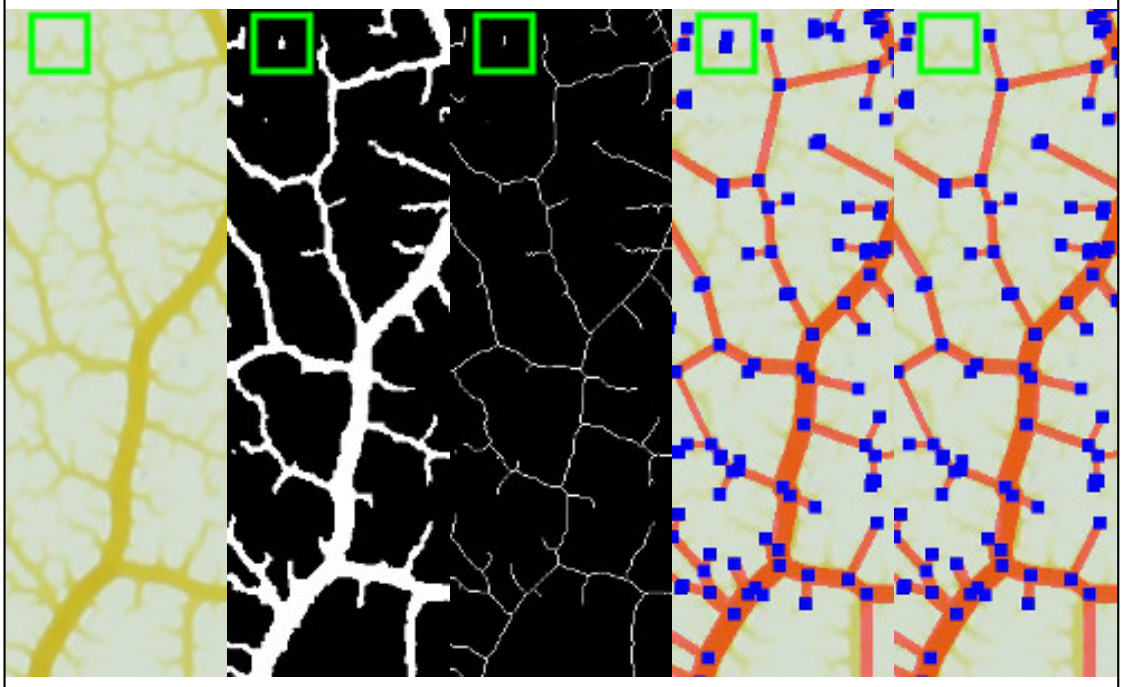

(a) Input image. (b) Segmented image. (c) Skeletonized image. (d) Detected graph drawn ontop of the input. (e) Filtered graph drawn ontop of the input.

Figure 1.2: Direct comparison of NEFI's pipeline steps given a slice of an image of a slime mold (*P. polycephalum*). From left to right: input image, segmented image, skeletonized image, detected graph and filtered graph. The green square contains a very faint vein which the segmentation did not pick up fully. Thus, the skeleton becomes fragmented which leads to spurious vertices in the detected graph. By applying a graph filter we remove stray vertices without manipulation of the segmented or the skeletonized image. Similar filtering can remove "dead-ends", i.e. vertices that do not belong to any cycle in the graph.

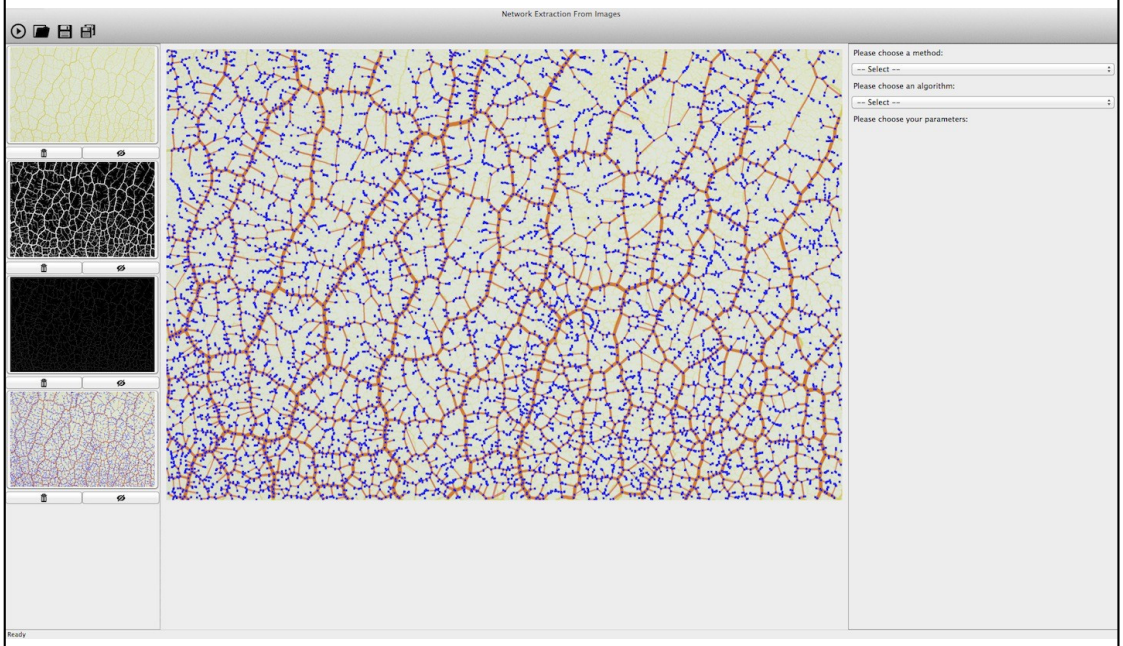

Figure 1.3: A screenshot of NEFI's GUI running on Mac OS. On the left hand side NEFI lists intermediate results as thumbnails. Bringing the final result to the center workspace allows for direct visual assessment of the quality of the extracted graph. On the right hand side NEFI's pipeline elements can be accessed via drop-down menus. The image was produced in a collaboration with the KIST Europe.

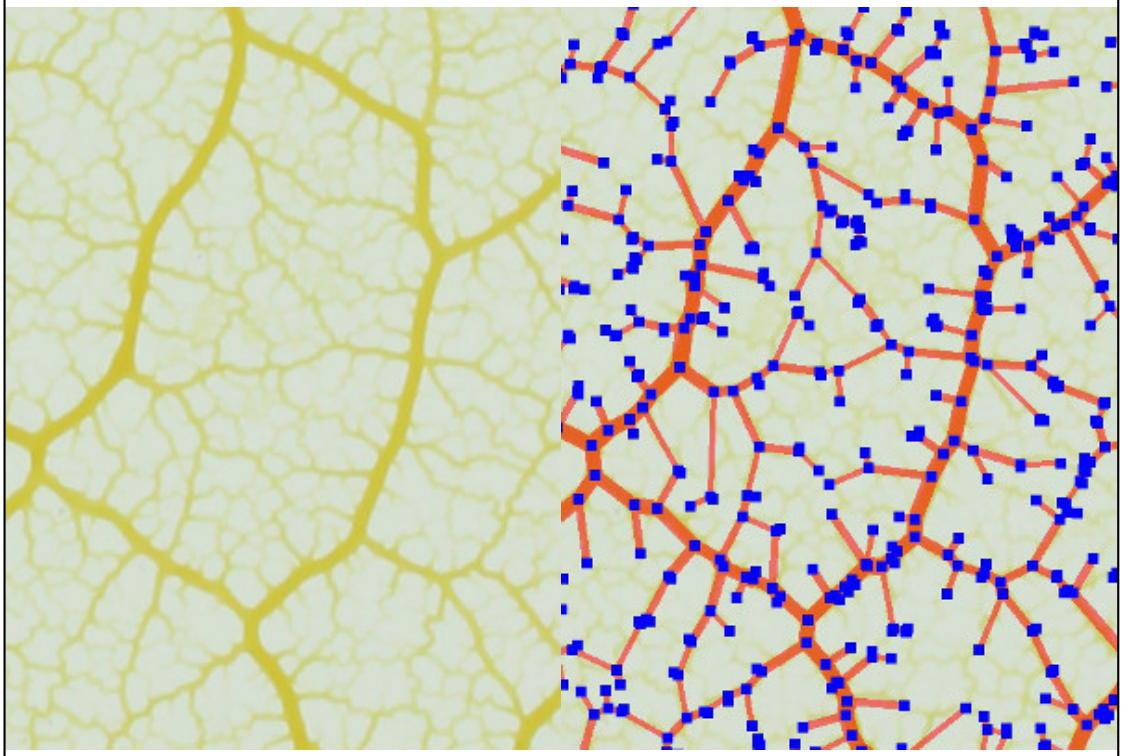

(a) (b)

Figure 1.4: Extracted graph of the network formed by a slime mold (*P. polycephalum*). The left hand side shows the input image depicting the network. The right hand side shows the extracted graph overlayed on top off the same image for direct comparison. Note, that no filters have been applied. The image was produced in a collaboration with the KIST Europe.

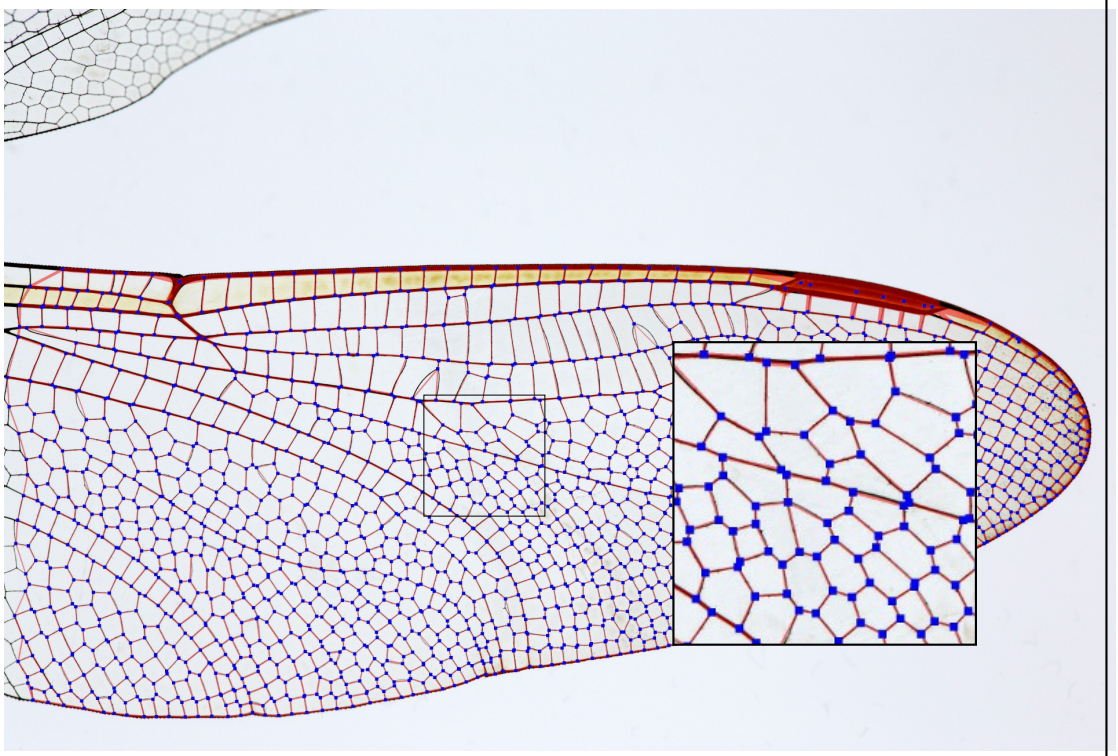

Figure 1.5: Extracted graph of the vein network exhibited by a wing of a dragonfly (*A. junius*). Note, that after the use of various filters a very clean-looking graph is obtained. Image courtesy of Pam and Richard Winegar.

by reducing the amount of spurious white pixels in the segmented image. However, blurring too much will remove fine detail and reduce accuracy in determining the thickness of depicted edges. As a result, we recommend to experiment with different approaches and parameter settings in order to decide how to use preprocessing. For images of sufficient quality we found that excellent results can be obtained without preprocessing.

NEFI relies on OpenCV [6] for preprocessing and offers Gaussian and Median Blurring, Denoising as well as Bilateral Filtering.

1.3.2 Segmentation Collection

The goal of the segmentation step is separating the image foreground, i.e. the structures of interest, from the remaining image. NEFI builds on top of OpenCV [6] combining different segmentation algorithms. The general-purpose algorithms shipped with NEFI have become standard in image processing and perform reliably well if input images are clean, devoid of strong gradients and have a good contrast between fore- and background. Conversely, if the input becomes more challenging, the effectiveness of NEFI's segmentation degrades quickly and more complex or domain-specific algorithms become necessary. We defer a quantitative study of how the properties of the input image affect NEFI's performance to the Section *Evaluation*.

NEFI's segmentation is designed such that several algorithms can be used interchangeably. We included basic thresholding algorithms like Otsu's method [1] or adaptive thresholding as well as more involved segmentation routines such as guided watershed [15] and the GrabCut algorithm [20]. The last two methods receive as an additional input a so-called marker. The better the markers approximate the foreground, the better these algorithms work. NEFI offers several marker strategies which can be used interchangeably together with the respective marker based segmentation routines.

Interchangeability of the algorithms is a core design principle of all pipeline steps.

This design facilitates easy experimentation with different methods. Our own experience shows that often it is not clear a priori which methods work for a given input image. This decision usually also depends on the desired degree of detail in the final output, where less sensitive methods might produce fewer false positives. This ease of experimentation with quick visual feedback from the GUI is one of the major strong points of NEFI.

The flexibility is not limited to the algorithms we provide. Instead, NEFI's software design makes it easy to integrate additional methods. We expect that in practice challenging inputs will be encountered for which the algorithms currently offered by NEFI will be insufficient. In these cases a potential user may choose

to implement additional, perhaps domain-specific, methods. By extending NEFI, the user can rely on existing modules and thus save a lot of time. The authors are convinced that improved extendability is another strong point of our work.

1.3.3 Graph Detection Collection

The graph detection collection consists of algorithms that take a segmented image as input and detect the nodes and the edges of the graph. We offer a colloquial description of the actual algorithm because we do not rely on well-documented library code for this section of the pipeline.

The first step for graph detection is called thinning. Here we reduce the segmented foreground such that every line is only one pixel thick, while preserving the connectivity properties of both the foreground and the background pixels. The result of this process is called the skeleton of the segmented image. To do so we implemented the algorithm by Guo and Hall [9]. It always produces thin results and preserves 8-connectivity of the foreground pixels. A pure Python implementation proved to be fairly slow, hence we chose to implement this function as a C extension.

For fairly thin foreground features this method is nearly flawless and finds a skeleton where the lines lie in the center of the foreground areas. However, large foreground sections lead to artifacts in the skeleton whose exact shape depends on the noise present at their borders.

On the skeleton we then detect the positions of nodes. For this purpose we adapt criteria from thinning algorithm by Zhang and Suen [24]. A white pixel becomes a node if its removal creates exactly one or at least three 4-connected white components in its 1-neighborhood. In the former case the pixel forms the end of a path, otherwise it is the meeting point of at least three edges.

Note that due to this step, the maximum degree of the graphs we detect is limited to four. This is inevitable if nodes are detected at single-pixel locations. For higher degree nodes we will create several nodes of limited degree that are very close to each other and can be merged by a later post-processing step.

Given the node positions, it is very simple to find the edges. We perform a variant of breadth first search on the white pixels in the skeleton, starting from each node simultaneously. Each white pixel around a node gets a unique number and a queue. In each step we iterate over all queues and take out the first pixel. If it is unmarked, we mark it with the unique number of this queue and enqueue all its white neighbors. Otherwise, we have detected an edge, i.e. there is a path along white pixels that connects two nodes.

While walking along the pixels we record the length of the edge. Horizontal and vertical steps count as one unit, diagonal steps count as $\sqrt{2} \approx 1.41$ units.

The diameter of an edge calculated by computing a distance transform on the

segmented image. This assumes that the thinned edge lies in the middle of the actual edge. Computing the diameters is now a simple lookup of each edge-pixel from the skeleton in the distance transformed image. As we have the diameters along the whole edge on hand by this procedure, we then compute a median and a variance.

For handling the graph we rely on NetworkX [11].

1.3.4 Graph Filter Collection

The graph filter collection offers the possibility to add powerful processing steps that directly apply to the graph obtained after graph detection.

Often it is possible to improve the result by removing unwanted artifacts in the segmented image or during later processing stages. A common strategy, used for example in [4], [5], consists of "reparing" the errors in the skeleton using heuristics or user assisted methods. However, these methods carry the potential danger of introducing additional errors.

NEFI pursues a novel approach by exploiting the structure of the extracted graph. First, we retain a maximum of structural information by not altering the segmented image or the skeleton at all, i.e. we establish the graph including all artifacts. Then we use dedicated graph filters to remove said artifacts. For example, if the network in the input image is reasonably large, it will result in a large connected component in the graph. Small components resulting from noise can thus be removed effectively and safely. Since the effects of filtering the graph can immediately be evaluated by visual inspection, we prefer graph filtering over less transparent approaches that take place before the graph was established. Figure 1.2 illustrates the use of filtering.

We have used filtering with sensitive segmentation to obtain surprisingly good results. Overly sensitive segmentation picks up fine detail but also introduces artifacts. However, almost all of the artifacts result in very small components that can easily be removed by filtering. The desired detail will remain mostly unaffected because it is part of the largest component. The graph depicted in Figure 1.5 was obtained using this technique.

Filtering may also be used to remove parts of the graph which are not of interest. The following filters are predefined in NEFI. A filter removing everything not in the largest connected component, one smoothing vertices of degree two except if this introduces parallel edges and finally, one which removes all vertices and edges that are not contained in a cycle. Filters may be freely combined in any order. Naturally, the filter collection is designed for extendability.

Graph filtering and its various applications delivers excellent results. To our knowledge, no other software offers such tools as part of its core workflow. For this reason, we consider this one of NEFI's strong points.

1.4 Evaluation

To assess NEFI's performance we investigate the output quality given input images of varying quality. Additionally we report on NEFI's speed.

1.4.1 Defining a Graph Similarity Measure

As a quality measure, we need to quantify the degree of congruence between the graph depicted in the original input image i and the graph computed by NEFI.

Let $A = (V_A, E_A)$ be the *true* graph correctly describing the structure depicted in i, with V_A and E_A denoting its vertex and edge set respectively. We call A the *ground truth*, which is of course not known in general. Furthermore, let B denote the graph obtained by executing one of NEFI's pipelines. Note that, $A, B \in \mathcal{G}$, where $\mathcal{G}$ denotes the set of undirected edge-weighted planar graphs where vertices are labeled with their respective euclidean coordinates in the plane. With these definitions we propose a similarity measure s mapping any pair of graphs $A, B \in \mathcal{G}$ onto a number $s \in [0, 1]$.

We compute a correspondence of vertices in A to vertices in B. Two edges $e \in E_A$ and $f \in E_B$ then correspond if their endpoints correspond. We choose the correspondence such that the following intuitive notion of similarity are optimized.

1. Positions of vertices in V_A are similar to positions of corresponding vertices in V_B.

2. Edges in E_A including their weights are similar corresponding edges in E_B.

For an exact definition of s and the notions of *similarity* and *correspondence*, we refer the reader to the supplementary material.

We require that the measure is maximal if any graph A is compared with itself, that is $s(A, A) = 1$. Consequently, if A is completely different from B we have $s(A, B) = 0$. This minimum value is assumed if no viable correspondence between V_A and V_B can be found. Naturally, the value of $s(A, B)$ increases (decreases) if the similarity between A and B increases (decreases).

1.4.2 Similarity Measure for Evaluation

In order to determine the overall quality of NEFI's output we need to quantify the degree of similarity between two graphs $A = (V_A, E_A)$ and $B = (V_B, E_B)$ using a graph similarity measure. Let $A, B \in \mathcal{G}$, where $\mathcal{G}$ is a set of undirected edges-weighted planar graphs where the nodes are labeled with their respective coordinates in the eucledian plane. Then we may define a similarity measure s as follows:

Connect this part to the next section instead ...

$$s : \mathcal{G} \times \mathcal{G} \to [0, 1] \tag{1.1}$$
$$\forall\ A, B \in \mathcal{G} : s(A, B) = matching(A, B) \tag{1.2}$$

Where $matching(A, B)$ denotes the normalized cost of a minimum cost graph matching problem which we will define shortly. Given this definition the degree of similarity between A and B is quantified by the value of $s(A, B)$. The similarity measure we propose has the following desirable properties:

- A compared to itself yields a maximum similarity score of $s(A, A) = 1$.
- If there are no vertices in V_A with corresponding similar nodes in V_B and no edges E_A with corresponding similar edges in E_B the minimum similarity score of $s(A, B) = 0$ is obtained.
- The similarity score $s(A, B)$ increases (decreases) if the similarity between A and B increases (decreases).

We proceed with making the notions of *similarity* and *correspondence* more precise by constructing a minimum cost graph matching problem. Given the two graphs $A, B \in \mathcal{G}$, let n_A, n_B denote the number of nodes and m_A, m_B denote the number edges of the respective graphs. Note that n_A and n_B can differ, as can m_A and m_B.

We can now define a matching between A and B consisting of three parts. First we define a matching between the node sets V_A, V_B, then we define a matching between the edges sets E_A, E_B and finally we introduce a coupling between the two. To obtain a solution to the problem we rephrase the combined matching problem as an integer linear program and solve it using IBM CPLEX. For ease of exposition, however, we discuss the problem using the language of matchings.

For the node matching, we match each node $i \in V_A$ with at most one node $j \in V_B$. We define a variable x_{ij} that is 1 if we match i with j and 0 otherwise. With a match we associate a cost of $\Delta_V(i, j)$. The function $\Delta_V(i, j)$ returns the euclidean distance between node i and node j. If any node u remains unmatched, we assign a penalty of $p_V(u)$ to it. A node can either be penalized or matched. We thus compute a minimum cost node matching, in which it is favorable for nodes in A to be matched with similar nodes in B. We call such a matching pair of similar nodes *corresponding*.

The edge matching proceeds analogously to the node matching. Each edge $e \in E_A$ is matched with at most one edge $f \in E_B$. We denote this match with a decision variable y_{ef} and associate a cost of $\Delta_E(e, f)$ with it. The function $\Delta_E(e, f)$ returns the sum of the differences in edge weights between edge e and

edge f. If any edge d remains unmatched, we assign a penalty of $p_E(d)$ to it. An edge can either be penalized or matched. We thus compute a minimum cost edge matching, in which it is favorable for edges in E_A to find a match with a similar edge in E_B. We call such a matching pair of similar edges *corresponding*.

As of yet both matchings are independent of each other. In particular this allows an edge e to be matched with an edge f independently from their respective positions in the plane as long as they have similar weights. A more meaningful matching favors pairing similar edges where the endpoints of both edges are similar to each other, i.e. geographically close. This additional constraint introduces a coupling between node and edge matching. To enforce coupling we add the constraint that an edge $e = (a, b) \in E_A$ can only be matched to an edge $f = (a', b')$ if the respective nodes participate in a matching as well. That is, we require a to be matched to a' and b to be matched to b' or alternatively a to be matched to b' and b to be matched to a'.

By combining node matching, edge matching and the additional coupling constraint we obtain the final minimum cost matching problem. We rephrase the uncoupled matching problem as an integer linear program (ILP) as follows:

$$minimize: \quad f = \sum_{\substack{i \in V_A \\ j \in V_B}} \Delta_V(i,j) x_{ij} \quad + \sum_{i \in V_A} p_V(i) \overline{x}_i + \sum_{j \in V_B} p_V(j) \overline{x}_j + \tag{1.3}$$

$$\sum_{\substack{e \in E_A \\ f \in E_B}} \Delta_E(e,f) y_{ef} + \sum_{e \in E_A} p_E(e) \overline{y}_e + \sum_{f \in E_B} p_E(f) \overline{y}_f \tag{1.4}$$

$$s.t.: \quad x_{ij} \in \{0,1\} \qquad i \in V_A \qquad j \in V_B \tag{1.5}$$

$$y_{ef} \in \{0,1\} \qquad e \in E_A \qquad f \in E_B \tag{1.6}$$

$$\forall\, i \sum_j x_{ij} \leq 1 \qquad \forall\, j \sum_i x_{ij} \leq 1 \tag{1.7}$$

$$\forall\, e \sum_f y_{ef} \leq 1 \qquad \forall\, f \sum_e y_{ef} \leq 1 \tag{1.8}$$

$$\overline{x}_i = 1 - \sum_{j \in V_B} x_{ij} \qquad \overline{x}_j = 1 - \sum_{i \in V_A} x_{ij} \tag{1.9}$$

$$\overline{y}_e = 1 - \sum_{f \in E_B} y_{ef} \qquad \overline{y}_f = 1 - \sum_{e \in E_A} y_{ef} \tag{1.10}$$

To introduce the coupling between the vertex and the edge matching, we add an additional constraint as described above:

$$\forall\, e = (a,b), f = (a',b'): \quad 2y_{ef} \leq x_{aa'} + x_{ab'} + x_{ba'} + x_{bb'} \tag{1.11}$$

Given the optimal solution to the ILP the optimal matching for nodes and edges can be recovered. Thus, we know what matching pairs have been formed and which nodes and edges remained unmatched. We use this information to define true positives, false positives and false negatives as described in the main manuscript.

In addition, we obtain the optimal value of the objective function OPT, i.e. the cost associated with the selected optimal matching. The value of OPT includes both the costs incurred by node and edge matches as well as the penalty terms arising from nodes and edges that cannot be matched. As a result it reflects the similarity between the two graphs A and B.

We point out that $OPT = 0$ if a graph G is matched with itself. Every single node and edge finds its exact copy as a match of cost 0 for itself and thus no penalties arise. The other extreme is realized when there are no vertices in V_A with corresponding similar nodes in V_B and no edges E_A with corresponding similar edges in E_B. In this case the value of OPT attains its maximum $\overline{OPT}$ because all nodes and edges of both graphs are penalized. Naturally, the value of OPT increases (decreases) with decreasing (increasing) graph similarity. Given these observations it is natural to use OPT and $\overline{OPT}$ to define a similarity measure betweens two graphs $A, B \in \mathcal{G}$ as follows

$$s(A,B) = matching(A,B) = 1 - \frac{OPT(A,B)}{\overline{OPT}(A,B)} \tag{1.12}$$

with

$$\overline{OPT}(A,B) = \sum_{i \in V_A} p_V(i) + \sum_{j \in V_B} p_V(j) + \sum_{e \in E_A} p_E(e) + \sum_{f \in E_B} p_E(f) \tag{1.13}$$

As a practical remark, we note that the number of variables entering the integer linear program grows like $\mathcal{O}(n_A n_B + m_A m_B)$. As a result, the linear program may become prohibitively large even for graphs of moderate size.

To meet this issue, it is convenient to define a circle with search radius r centered around each node i. Our goal is to exclusively consider nodes j within this search radius to consider as possible matches for node i. In other words, we label all nodes j outside the search circle as too expensive. To correctly enforce this idea in the integer linear program, we require $p_V(u) > r$ for all nodes u in both graphs.

With this definition in place, none of the nodes j outside of the search circle will be selected as an optimal match for node i because two nodes i and j are matched if and only if the cost of forming the pair is smaller than the penalty due

Fix the
and feel
chapter,
cially wh
it comes
maths . .

for payment in case the match is not established. Thus, the respective variables x_{ij} may safely be omitted from the linear program.

Choosing the search radius and adjusting the penalties accordingly in order to control the size of the linear program seems more natural to the authors than the other way around. This approach has the additional advantage that a sensible value for the search radius can often be inferred by the looking at the length scales of the structures of interest in the original input image.

The number of variables y_{ef} referring to edge pairs can be reduced by separately applying the previous argument to each of the nodes involved. We enumerate the set of all possible edges $f = (a', b')$ to be matched with edge $e = (a, b)$. The edges $f = (a', b')$ are constructed by connecting all nodes a' within a radius r around the node a with all nodes b' within a radius r around node b. This process can create self-loops $f = (a', a')$ which we exclude as candidates. If there are no nodes within a distance r from a or b, the associated edge variables y_{ef} can be omitted from the linear program. To correctly enforce this idea in the ILP, we normalize the cost of the edges associated with the variables y_{ef} and choose the edge penalties as $p_E(d) > r$ for all edges d in both graphs. There is considerable freedom in the choice of the edge penalties as long as they are large enough that sensible matches y_{ef} are not ignored in favor of paying cheaper penalties.

It is advised to experiment with different values or to simply choose them larger than the largest edge match cost. The latter choice has the effect that whenever a match is available it will be selected, even if the cost is extremely large. As a result this choice is justified in particular when the edge costs are known to be comparable in magnitude. As a concluding remark, we stress that the choice of penalties for nodes and edges affects the final value of the similarity measure $s(A, B)$ via the normalization. As a result, when using this measure to compare several graphs with each other, the penalties and tracking radius r must be chosen consistently in order to guarantee the viability of the comparison.

1.4.3 Evaluation of NEFI's Output

We proceed with the evaluation of NEFI's output using the above similarity measure. To do so we create a set $\mathcal{A}$ of ground truth graphs such that $\mathcal{A} \subset \mathcal{G}$. We start by processing a real-life set I_0 of images of the slime mold *P. polycephalum* with NEFI. Thus we obtain a set of graphs $\mathcal{B}_0 \subset \mathcal{G}$. Given those graphs we obtain the set $\mathcal{A}$ by distorting the graphs $B_i \in \mathcal{B}_0$ using different graph filters. At this point we will not use the images in I_0 or the graphs in $\mathcal{B}_0$ anymore.

Next, we turn the graphs in $\mathcal{A}$ into a test set I_1 of 2D images by simply drawing them. The drawing preserves the euclidean positions of the nodes, the edge lengths and the thickness of the edges. As a result, the image $i \in I_1$ depicts the graph $A_i \in \mathcal{A}$. In other words, we know the *ground truth* A_i for every image i in the test

set I_1.

To compare different segmentation methods, we prepare a set $\mathcal{P}$ of pipelines differing only in the segmentation algorithms used. The parameters of the pipeline where chosen manually for each test set using experimentation and visual inspection.

Given the sets I_1 and $\mathcal{A}$ as well as our similarity measure we can now evaluate NEFI's output. We take an image $i \in I_1$ and process it with a given $p \in \mathcal{P}$ to obtain a graph $B_i \in \mathcal{B}_1$, i.e. the graph NEFI extracted from the input image. Then we compute the similarity $s(A_i, B_i)$. To obtain statistical statements, we repeat this procedure for all images and all pipelines.

During the computation of $s(A_i, B_i)$, we record features NEFI failed to detect in i, namely the number of vertices (edges) in A_i which remain without corresponding vertices (edges) in B_i. This is the number of false negatives (FN). Furthermore, we record the number of vertices (edges) in B for which no corresponding vertices (edges) exist in A_i. These are features which NEFI detects in i but which are in fact not present. These are false positives (FP). Finally we record the number of vertices (edges) in B_i that have corresponding elements in A_i. That is, features correctly extracted from the image i, which we count as true positives (TP). Unfortunately, we cannot determine the number of true negatives (TN) in a similar fashion. For this reason we restrict ourselves to computing sensitivity ($\frac{TP}{TP+FN}$) and precision ($\frac{TP}{TP+FP}$) in the results of the evaluation. Sensitivity and precision reported in the following Tables combine the respective values for vertices and edges.

Table 1.1 summarizes the results of processing the set I_1. The images in I_1 are ideal inputs for NEFI for which all our segmentation routines produce very good results. Otsu's method and adaptive thresholding yield perfect segmentations. Hence, any difference between NEFI's output and the ground truth cannot originate in the segmentation part of the pipeline but must be attributed to thinning and graph detection. The excellent correspondence between NEFI's output and the ground truth confirms that thinning and graph detection are very reliable.

Fix the look of these tables ...

One might question the validity of using graphs which were detected by NEFI in the first place as the input set. However, the approach is valid because the origin of the images in I_1 has no significance regarding NEFI's performance. In other words, they are just as hard or as easy to process as images obtained in any other comparable way.

The perfect images in I_1 do not represent real life input very well. Therefore we produced three more test sets and evaluate them as described above.

For the set I_2 we take the images in I_1 and change the brightness of the edge drawings randomly. As a result the local contrast between foreground and background varies widely across the image. To create set I_3 we take the images in

Method	Similarity score s	Sensitivity	Precision
Otsu's method	0.984 ± 0.005	0.970 ± 0.011	0.998 ± 0.001
Adaptive threshold	0.984 ± 0.005	0.970 ± 0.011	0.997 ± 0.001
Watershed (deletion/erosion)	0.980 ± 0.006	0.959 ± 0.013	0.988 ± 0.001
Watershed (distance transform)	0.906 ± 0.121	0.837 ± 0.160	0.998 ± 0.001
Watershed (adaptive)	0.977 ± 0.008	0.956 ± 0.016	0.998 ± 0.001
Grabcut (deletion/erosion)	0.984 ± 0.005	0.970 ± 0.011	0.998 ± 0.001
Grabcut (distance transform)	0.983 ± 0.005	0.967 ± 0.011	0.998 ± 0.001

Table 1.1: Summary of the evaluation of 250 ideal test images I_1.

Method	Similarity score s	Sensitivity	Precision
Otsu's method	0.868 ± 0.018	0.704 ± 0.028	0.987 ± 0.005
Adaptive threshold	0.941 ± 0.010	0.853 ± 0.034	0.976 ± 0.025
Watershed (deletion/erosion)	0.859 ± 0.018	0.693 ± 0.028	0.984 ± 0.006
Watershed (distance transform)	0.408 ± 0.176	0.239 ± 0.154	0.987 ± 0.007
Watershed (adaptive)	0.966 ± 0.008	0.936 ± 0.016	0.984 ± 0.017
Grabcut (deletion/erosion)	0.864 ± 0.019	0.696 ± 0.029	0.986 ± 0.005
Grabcut (distance transform)	0.858 ± 0.020	0.688 ± 0.030	0.986 ± 0.005

Table 1.2: Summary of the evaluation of 250 test images I_2 with edges drawn with random brightness.

I_1 and insert a color gradient into the background while leaving the foreground unchanged. Set I_4 is obtained by taking the images in I_1 and subjecting them to a global blur.

Table 1.2 summarizes the results of processing the set I_2. We observe that both similarity score as well sensitivity are deteriorating for almost all methods except for adaptive thresholding and watershed based on adaptive thresholding. Adaptive thresholding is still able to compensate the local changes in brightness present in the test images and returns segmented images of high quality. We stress that for images showing more severe irregularities the performance of these methods is expected to suffer.

Note that the precision remains comparably high, which indicates that the vertices and edges detected by NEFI are indeed part of the ground truth.

Table 1.3 summarizes the results of processing the set I_3. We observe that almost all methods, with the exception of adaptive thresholding and watershed based on adaptive thresholding perform very poorly. In particular watershed based on a distance transform marker is completely unable to handle the input images.

Method	Similarity score s	Sensitivity	Precision
Otsu's method	0.737 ± 0.060	0.602 ± 0.065	0.911 ± 0.065
Adaptive threshold	0.984 ± 0.005	0.970 ± 0.011	0.998 ± 0.001
Watershed (deletion/erosion)	0.752 ± 0.047	0.588 ± 0.061	0.977 ± 0.009
Watershed (distance transform)	0.334 ± 0.303	0.240 ± 0.261	0.943 ± 0.043
Watershed (adaptive)	0.982 ± 0.005	0.967 ± 0.012	0.997 ± 0.001
Grabcut (deletion/erosion)	0.733 ± 0.053	0.573 ± 0.066	0.987 ± 0.005
Grabcut (distance transform)	0.742 ± 0.052	0.582 ± 0.065	0.983 ± 0.008

Table 1.3: Summary of the evaluation of 250 test images I_3 with a color gradient in the background.

Method	Similarity score s	Sensitivity	Precision
Otsu's method	0.953 ± 0.011	0.909 ± 0.022	0.993 ± 0.003
Adaptive threshold	0.947 ± 0.010	0.863 ± 0.028	0.989 ± 0.005
Watershed (deletion/erosion)	0.950 ± 0.010	0.915 ± 0.022	0.981 ± 0.010
Watershed (distance transform)	0.738 ± 0.127	0.575 ± 0.147	0.915 ± 0.059
Watershed (adaptive)	0.954 ± 0.010	0.909 ± 0.329	0.975 ± 0.020
Grabcut (deletion/erosion)	0.950 ± 0.012	0.903 ± 0.024	0.993 ± 0.003
Grabcut (distance transform)	0.918 ± 0.024	0.838 ± 0.046	0.990 ± 0.004

Table 1.4: Summary of the evaluation of 250 blurred test images I_4.

Table 1.4 summarizes the results of processing the set I_4. We observe that almost all methods, with the exception of watershed with distance transform, perform reasonably well. Sensitivity and similarity scores are slightly smaller than the results obtained for the optimal test images I_1. This is due to the fact that blurring an image i causes the depicted edges to appear slightly wider. This increase in width is detected in the edges of the graphs B_i. As a result the similarity score $s(A_i, B_i)$ decreases accordingly.

Summarizing the results we conclude that the quality of a graph detected by NEFI depends on the input image and the selected pipeline. We have established that the major factor determining the quality of the extracted graph is indeed the segmentation step. Errors introduced by thinning and graph detection appear negligible in comparison.

Consequently, NEFI's major limitations arises from the limited applicability of its the segmentation algorithms. As a result, NEFI operates best on clean and uncluttered images such as images produced under controlled laboratory conditions. More difficult input may still be processed, possibly at the cost of reduced qual-

Pipeline element	Image small (1152 × 864)	Image large (5760 × 3840)
Watershed	< 1	2
GrabCut	6	160
Adaptive threshold	< 1	7
Guo-Hall thinning	< 1	12
Vertex detection	< 1	5
Edge detection	< 1	6
Computing edge weights	< 1	5

Table 1.5: Timings of some of NEFI's pipeline elements on images of different size. All values are in seconds. The timings were obtained on a Macbook Pro notebook equipped with a 2.4 GHz Intel i5 processor and 8 GB RAM.

ity. For these inputs, domain specific algorithms might be necessary and can be implemented as extensions for NEFI. Alternatively, the segmentation step can be entirely outsourced to more specialized third-party software. Given the externally segmented image as an input, NEFI's pipeline may proceed directly with graph detection.

We refer the reader to the Supplementary Material for a short guide that summarizes our experience when dealing with more challenging input.

1.4.4 Evaluation of Speed Performance

NEFI was designed to efficiently process large quantities of images. Thus it outsources computationally intensive tasks to highly optimized and reliable libraries such as Itseez, OpenCV [6] and NetworkX Developer Team, NetworkX [11]. Table 1.5 illustrates the effectiveness of some of NEFI's algorithms.

1.5 Limitations of NEFI

In the last section we have seen how the quality of the extracted graph changes depending on the input image and the selected segmentation algorithms. We have established that the major factor determining the quality of the extracted graph is indeed the segmentation step. As a result NEFI's major limitation naturally arises from the limited domain of effectiveness of NEFI's general purpose segmentation collection. It's methods do not work very well if the input contains irregular background or color/brightness gradients, has low contrast or insufficient resolution to detect structures that are either too dense or too fine. For these inputs, domain specific algorithms are necessary and should be implemented as extensions for

NEFI. Alternatively, the segmentation step can be entirely outsourced to more specialized third-party software. Given the externally segmented image as an input NEFI's pipeline may proceed directly with graph detection.

In general, however, NEFI's domain of effectiveness is limited to sufficiently clean and uncluttered images such as images produced under controlled laboratory conditions. We refer the reader to the supplementary material for a short trouble-shooting guide that summarizes our experience when dealing with more challenging input.

Another limitation arises due to the nature of NEFI's vertex detection. Since we walk the skeleton in search junctions, no vertices of degree two are detected. Furthermore, vertices of high degree (4 or more) are split into several degree three vertices. The latter can be undone by merging vertices using a suitable graph filter.

As a concluding remark, we stress that NEFI tries to compensate some of its limitations by offering the possibility to work with segmented images from other sources or to integrate additional algorithms with comparably little effort. NEFI should be regarded as a flexible platform suitable for further development rather than a universal solution to the network extraction problem.

1.6 Synergies With Other Software

1.6.1 Analysis of Graphs

NEFI is a tool that facilitates data acquisition, which is a necessary precursor to data analysis. To analyze NEFI's output one can either rely on open source graph analysis software [2], [3], [10], [13], [14], [23] or write custom programs. NEFI can output many common graph formats, readable by most popular graph libraries. To get the user started immediately, we provide a minimal Python program that illustrates the basic steps required to perform graph analysis. It shows how to read NEFI's output from disk and how to compute a histogram of a given edge attribute. The code can be downloaded from NEFI's project page at the Max Planck Institute for Informatics, http://nefi.mpi-inf.mpg.de.

1.6.2 Third-party Segmentation Software

NEFI's graph detection takes a segmented image as an input. Such an image need not be produced by using NEFI but can be obtained by relying on arbitrary third-party segmentation algorithms or tools.

In this context an interesting tool called ilastik [22] was brought to our attention. ilastik offers a so-called *classification workflow* in which a pixel classifier is trained by interactive user inputs. The trained classifier can then be used to automatically

segment previously unseen images. The segmented images obtained in this way can then directly be turned into graphs using NEFI.

By using NEFI in conjunction with third-party software the benefits of both can be realized.

1.7 Discussion

We anticipate NEFI to become a valuable tool that allows scientists from any domain to automate graph extraction from images in an intuitive fashion requiring no expert knowledge. We hope that researchers will be able to spend more time on analyzing their data and less time on processing it. By providing a flexible platform for graph extraction, we invite experts to extend and improve NEFI in order to introduce their contributions to a wider interdisciplinary audience. In the long run we would like NEFI to further the field of network science by promoting the creation of new network databases.

1.8 Acknowledgments

We thank Prof. M. Hauser for sparking our interest in this topic. We thank Prof. K. Mehlhorn for supporting this project with valuable comments and encouragement. We thank P. and R. Winegar as well as the Korea Institue of Science and Technology Europe for contributing sample data. This work was supported by the Max Planck Institute for Informatics and the IMPRS Saarbrücken.

1.8.1 General Information about NEFI

NEFI is an open source Python application and available at its project page at Max Planck Institute for Informatics, http://nefi.mpi-inf.mpg.de. NEFI's homepage includes a gallery of various use-cases and a comprehensive guide containing instructions on how to download, install and use NEFI on Windows, Mac and Linux. Additionally, a supplementary datasets is available for download there, allowing for a quick evaluation of NEFI's main features. This dataset can be used to reproduce the figures and evaluation results shown in this manuscript.

Bibliography

[1] "A threshold selection method from gray-level histograms", *Systems, Man and Cybernetics, IEEE Transactions on*, vol. 9, no. 1, pp. 62–66, Jan. 1979, ISSN: 0018-9472. DOI: 10.1109/TSMC.1979.4310076.

[2] M. Bastian, S. Heymann, and M. Jacomy, "Gephi: an open source software for exploring and manipulating networks", 2009. [Online]. Available: http://www.aaai.org/ocs/index.php/ICWSM/09/paper/view/154.

[3] V. Batagelj and A. Mrvar, "Pajek-program for large network analysis", *Connections*, vol. 21, no. 2, pp. 47–57, 1998.

[4] W. Baumgarten and M. J. Hauser, "Detection, extraction, and analysis of the vein network", *Journal of Computational Interdisciplinary Sciences*, vol. 1, no. 3, pp. 241–249, 2010.

[5] ——, "Computational algorithms for extraction and analysis of two-dimensional transportation networks", *J. Comput. Interdiscip. Sci*, vol. 3, pp. 107–16, 2012.

[6] G. Bradski, "The OpenCV Library", *Dr. Dobb's Journal of Software Tools*, 2000.

[7] D. Chai, W. Forstner, and F. Lafarge, "Recovering line-networks in images by junction-point processes", in *Computer Vision and Pattern Recognition (CVPR), 2013 IEEE Conference on*, IEEE, 2013, pp. 1894–1901.

[8] M. T. Dehkordi, S. Sadri, and A. Doosthoseini, "A review of coronary vessel segmentation algorithms", *Journal of medical signals and sensors*, vol. 1, no. 1, p. 49, 2011.

[9] Z. Guo and R. W. Hall, "Parallel thinning with two-subiteration algorithms", *Communications of the ACM*, vol. 32, no. 3, pp. 359–373, 1989.

[10] A. A. Hagberg, D. A. Schult, and P. J. Swart, "Exploring network structure, dynamics, and function using NetworkX", in *Proceedings of the 7th Python in Science Conference (SciPy2008)*, Pasadena, CA USA, Aug. 2008, pp. 11–15.

[11] ——, "Exploring network structure, dynamics, and function using NetworkX", in *Proceedings of the 7th Python in Science Conference (SciPy2008)*, Pasadena, CA USA, Aug. 2008, pp. 11–15.

[12] M. Krause, R. M. Alles, B. Burgeth, and J. Weickert, "Fast retinal vessel analysis", *Journal of Real-Time Image Processing*, pp. 1–10, 2013.

[13] J. Leskovec and R. Sosič, *SNAP: a general purpose network analysis and graph mining library in C++*, http://snap.stanford.edu/snap, Jun. 2014.

[14] S. Loscalzo and L. Yu, "Social network analysis: tasks and tools", in *Social computing, behavioral modeling, and prediction*, Springer, 2008, pp. 151–159.

[15] F. Meyer, "Un algorithme optimal pour la ligne de partage des eaux", *Dans 8me congrès de reconnaissance des formes et intelligence artificielle*, vol. 2, pp. 847–857, 1991.

[16] M. Negri, P. Gamba, G. Lisini, and F. Tupin, "Junction-aware extraction and regularization of urban road networks in high-resolution sar images", *Geoscience and Remote Sensing, IEEE Transactions on*, vol. 44, no. 10, pp. 2962–2971, Oct. 2006, ISSN: 0196-2892. DOI: 10.1109/TGRS.2006.877289.

[17] M. Newman, "The structure and function of complex networks", *SIAM Review*, vol. 45, no. 2, pp. 167–256, 2003. DOI: 10.1137/S003614450342480. eprint: http://dx.doi.org/10.1137/S003614450342480. [Online]. Available: http://dx.doi.org/10.1137/S003614450342480.

[18] B. Obara, M. Frickerc, and V. Graua, "Contrast independent detection of branching points in network-like structures", in *SPIE Medical Imaging*, International Society for Optics and Photonics, 2012, pp. 83141L–83141L.

[19] B. Obara, V. Grau, and M. D. Fricker, "A bioimage informatics approach to automatically extract complex fungal networks", *Bioinformatics*, vol. 28, no. 18, pp. 2374–2381, 2012.

[20] C. Rother, V. Kolmogorov, and A. Blake, "Grabcut - interactive foreground extraction using iterated graph cuts", *ACM Trans. Graphics (SIGGRAPH)*, pp. 309–314, 2004.

[21] E. Samuel, C. de la Higuera, and J.-C. Janodet, "Extracting plane graphs from images", English, in *Structural, Syntactic, and Statistical Pattern Recognition*, ser. Lecture Notes in Computer Science, E. R. Hancock, R. C. Wilson, T. Windeatt, I. Ulusoy, and F. Escolano, Eds., vol. 6218, Springer Berlin Heidelberg, 2010, pp. 233–243, ISBN: 978-3-642-14979-5. DOI: 10.1007/978-3-642-14980-1_22. [Online]. Available: http://dx.doi.org/10.1007/978-3-642-14980-1_22.

[22] C. Sommer, C. Straehle, U. Köthe, and F. A. Hamprecht, "Ilastik: interactive learning and segmentation toolkit", in *2011 IEEE international symposium on biomedical imaging: From nano to macro*, IEEE, 2011, pp. 230–233.

[23] K. Xu, C. Tang, R. Tang, G. Ali, and J. Zhu, "A comparative study of six software packages for complex network research", in *Communication Software and Networks, 2010. ICCSN '10. Second International Conference on*, Feb. 2010, pp. 350–354. DOI: 10.1109/ICCSN.2010.34.

[24] T. Zhang and C. Y. Suen, "A fast parallel algorithm for thinning digital patterns", *Communications of the ACM*, vol. 27, no. 3, pp. 236–239, 1984.

Todo list